Journal of Advanced Research in Fluid Mechanics and Thermal Sciences

Journal homepage:
https://semarakilmu.com.my/journals/index.php/fluid_mechanics_thermal_sciences/index
ISSN: 2289-7879

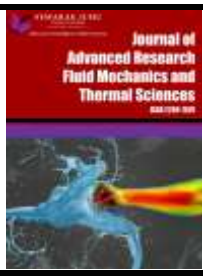

Creating and Simulating Turbulence Generation on NACA S1046 Airfoil with CFD Software

Erwin Erwin[1,2,*], Muhammad Syihab Fachry[1], Slamet Wiyono[1,2], Bima Heska Putra[2], Edy Susanto[3], Anwar Ilmar Ramadhan[3], Wan Hamzah Azmi[4]

[1] Mechanical Engineering Department, Universitas Sultan Ageng Tirtayasa Jl. Jenderal Sudirman Km 3, Purwakarta, Cilegon, Indonesia
[2] Renewable Energy Design Laboratory, Universitas Sultan Ageng Tirtayasa Jl. Jenderal Sudirman Km 3, Purwakarta, Cilegon, Indonesia
[3] Department of Mechanical Engineering, Institut Teknologi PLN, Jakarta 11750, Indonesia
[4] Faculty of Mechanical and Automotive Engineering Technology, Universiti Malaysia Pahang Al-Sultan Abdullah, 26600 Pekan, Pahang, Malaysia

ARTICLE INFO

Article history:
Received 23 April 2024
Received in revised form 13 July 2024
Accepted 22 July 2024
Available online 15 August 2024

Keywords:
Airfoil; boundary layer; fluid; flow separation; turbulator

ABSTRACT

The efficiency of wind turbines according to Betz limits ranges around 59%, in its development the efficiency of wind turbines is challenging to reach 50%. To increase this efficiency, many innovations were made such as the addition of tail direction, wind direction, the use of magnetic bearings, and turbulators. Flow separation that occurs in the blade causes a decrease in performance in the blade, which also occurs in vertical wind turbine blades. This research used a turbulator to reduce or shift the position of separation on the blade to improve turbine efficiency. This study aims to analyze the effectiveness of the use of turbulators to reduce or shift separation in wind turbine blades. The method used is to build a 3d model of the blade and turbulator, and perform simulations using CFD Ansys, with a steady flow with k-w Shear Stress Transport (k-w SST) turbulent model, at several speeds and angles of attack. The data taken is flow data on the blade, drag coefficient, and lift coefficient. When a turbulator is introduced, the results show a discernible delay in flow separation on the airfoil, namely at angles of 6°, 7°, and 8° with speeds ranging from 1 to 5 m/s. Furthermore, changes in the values of Cl and CD are noted. Pressure distribution contours and streamlines are graphically represented alongside the current numerical values. The optimal placement for the turbulator is at 40% and 50% of the chord length, producing the greatest increase in Cl and Cl/Cd ratio in this particular version.

1. Introduction

Wind energy is one of the energies that includes alternative energy and has the potential to be developed in the future. Wind energy includes clean and renewable energy. The wind is the air that moves due to the rotation of the earth and the difference in atmospheric pressure around it. A study of flow-separation is among the difficulties with turbomachinery [1]. In axial compressors, 50% of energy losses qualitatively result from flow separation, and the remaining is split into two categories:

* *Corresponding author.*
E-mail address: erwin@untirta.ac.id

https://doi.org/10.37934/arfmts.120.1.98110

frictional losses and losses resulting from changes in size or form [2]. The worst consequence of this flow separation phenomenon is that it can cause an adverse pressure gradient to cause a wake phenomenon, an area behind which has a different speed from the free stream velocity. The wake phenomenon can increase drag and cause stall, a condition where the airfoil loses lift and a very large drag increase [3].

Based on these facts, improving the performance of the turbomachinery can be started by overcoming this flow separation. It is known that the boundary layer with more turbulence (higher turbulence intensity), always produces a higher, more complete momentum profile so that the energy flow is stronger. Consequently, to improve the flow's ability to withstand adverse pressure, flow separation reduction can be achieved by making the flow more turbulent (back pressure) [4,5].

In the aeronautical field, the turbulator is known to be used in certain flight conditions as a passive flow control device that makes the flow at the boundary layer turbulent. This turbulent condition will slow down the flow separation point (airfoil stall condition) and increase the stall angle of attack [6]. Reducing the turbulent wake intensity behind the trailing edge fringe increases aerodynamic performance in Serrated Wings, taken from Uppu and Krishnan [7].

Research related to the addition of a turbulator/vortex generator on an airfoil Eppler 387 type, and the results obtained that there was an increase in the lift coefficient; there was also a decrease and increase in the drag coefficient at different angles of attack and also fluctuations in the value of the Cl/Cd ratio according to Delnero *et al.,* [8,9]. Previous research by Lin [10] that implements turbulators on blades has been mostly done on horizontal turbines and shows that using a turbulator causes a delay in the separation of the flow, but research using turbulators on vertical turbine blades such as Darrieus turbines is nothing yet, mainly focuses on wind steering devices by Erwin *et al.,* [11], and tail implementation by Lusiani *et al.,* [12]. According to Henrik and Soeren [13], the turbulator can also function to dampen vibrations that occur in the blade when rotating at high speeds.

In a previous study, we built a fluid flow simulation system using smoke to obtain flow visualization in the wind tunnel in testing the NACA S1046 blade, it was seen that the flow separation happened at an angle of 7° so further action was needed to reduce the flow separation phenomenon.

The novelty of the present study can be summarized as follows

i. Overcome the flow separation phenomenon by using a turbulator that is used in the vertical wind turbine, the Darrieus type, with the NACA S1046 blade.
ii. Numerical methods / CFD simulation (computer fluid dynamics) along with analysis of the drag coefficient and lift coefficient. Using the Ansys Fluent software, a simulation of the airfoil and turbulator shows they affect flow separation.
iii. The optimum configuration offered is based on performance that increases up to 40%.

2. Related Works

This research was conducted by designing and testing 3D (three-dimensional) numerical methods. To do the simulation, the CFD application Ansys Fluent is used. The models designed are airfoils and airfoils with the addition of a turbulator/vortex generator.

Modeling is done using Ansys Design Modeler. The simulation conditions used are at speeds of 1 to 5 m/s with angles of attack 6°, 7°, and 8°. The turbulator configuration is adjusted for distance with 5 variations based on chord length, namely 10%, to 50% chord calculated from the leading edge. The flow conditions used are steady and incompressible, the fluid (air) coming through the inlet section parallel to the axis direction. The airfoil used is the NACA S1046 type which can be seen in Figure 1 and the configuration of the trapezoidal flat plate counter rotating turbulator with fillet modification can be seen in Table 1.

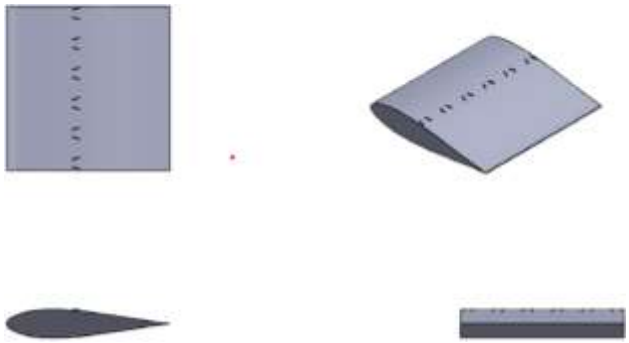

Fig. 1. Airfoil model

In the picture, a turbulator is applied in one of the variations of its placement, namely at the placement of 30% Chord length (counting from the leading edge point parallel to the x-axis). Furthermore, there is a table detailing the configuration and dimensions of the airfoil and turbulator.

Table 1
Airfoil and Turbulator Configuration

Airfoil NACA S1046	Turbulator
Chord (*C*) = 1000 mm	Height 1 (H1) = 0,0086C
Span (*S*) = 1000 mm	Height 2 (H2) = 0,0043C
Max Thickness (*T*) = 46mm	Turbulator Direction to Chord = 10%C, 40%C and 50%C from *leading edge*
Angle of Attack = 6°, 7°, 8°	Turbulator Direction to Span = 8,19 mm
	Length (*l*) = 0,0455C
	Width (*w*) = 0,0027C
	Tilt Angle = 18°
	Distance Between Turbulator 45,5mm
	Distance Between Each set Turbulator's (from the center) 182mm

Based on the configuration above, the details can be seen in Figure 2.

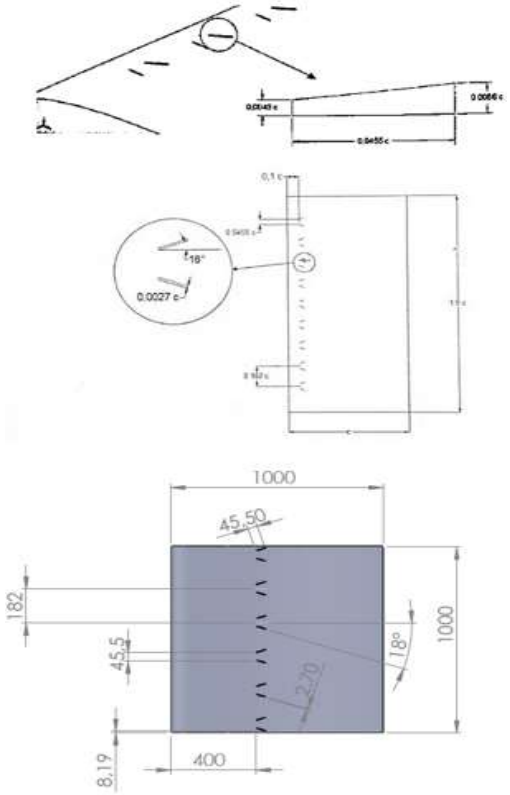

Fig. 2. Airfoil and turbulator configuration

3. Proposed Methodology

The simulation carried out in three stages, that is

i. Pre-Processing

At this stage, the airfoil model along with the turbulator designed using Ansys Design Modeler. At this stage, it is further divided into several sub-stages, namely the design of the airfoil and turbulator models, modeling/domain simulation, meshing, and determination of boundary conditions. The condition of the simulation domain and the state after meshing (with the form of polyhedral meshing) can be seen in Figure 3 and Figure 4.

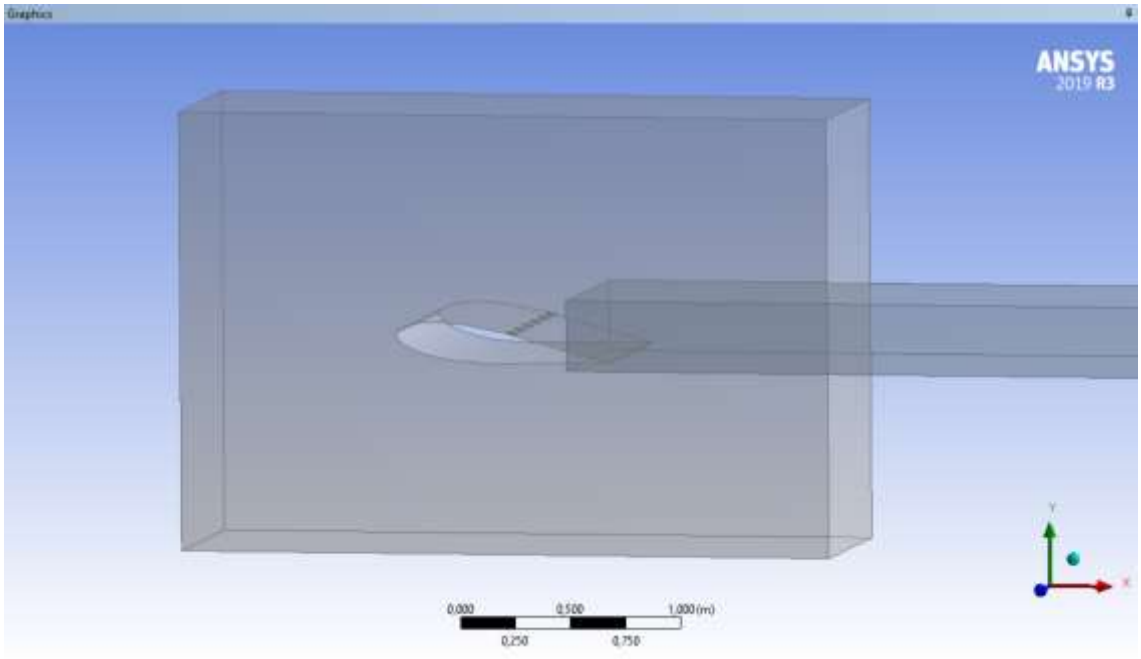

Fig. 3. Simulation domain model

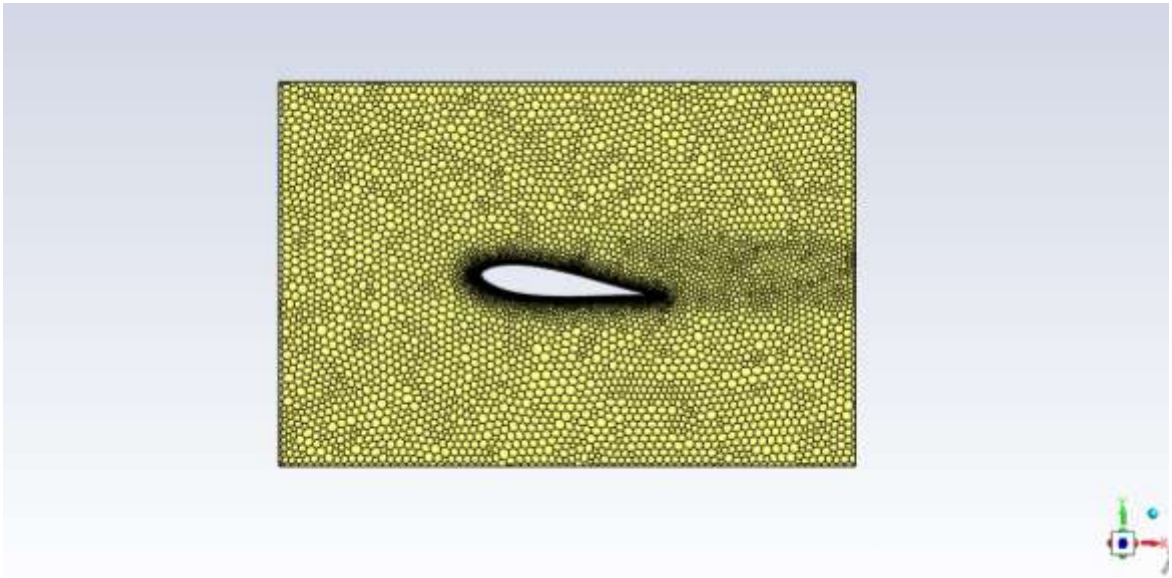

Fig. 4. Meshing

Furthermore, the details of the boundary conditions applied to the model domain that apply the same system to the wind (wind tunnel) in real conditions can be seen in Figure 5. Dimensions of the simulation domain were set as 17000mm × 9660mm × 1000 nm in the lateral (x), vertical (y), and longitudinal (z) directions, respectively.

The mesh type used is poly-hedral with the total number of cells being 780800 after mesh independency test of Cd and Cl. The resulting mesh quality is quite good with a maximum skewness of 0.8 and a minimum orthogonal quality of 0.12 (Ansys mesh metric recommendation, maximum orthogonal > 0, and maximum skewness < 0.95, depending on physics and cell location).

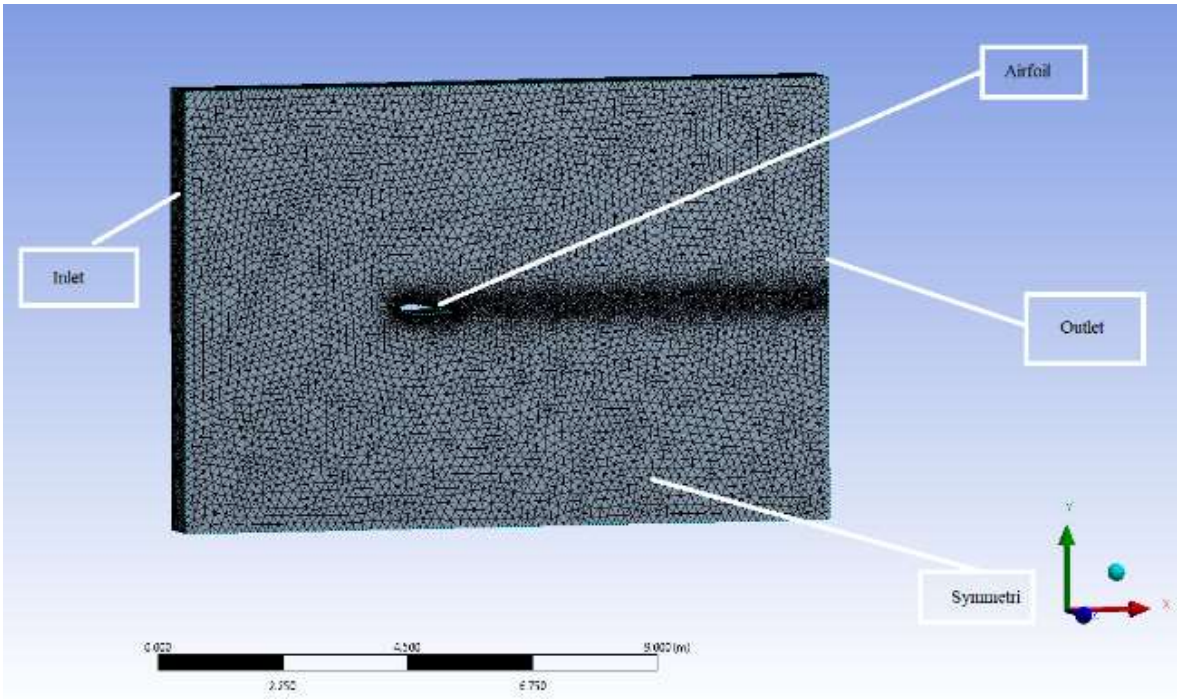

Fig. 5. Boundary condition applied to the domain

ii. Processing

At this stage, a calculation (iteration) will be carried out on Ansys based on predetermined condition parameters, namely the Turbulence model used is k-ω SST taken from Muratoğlu and Demir [14] and Rocha *et al.,* [15] (taking into account that k- SST is a combination of standard k-omega which is stable and accurate in the region near the wall and the k-epsilon model which has advantages in free-stream flow) with the material property of being fluid with = 1,225 kg m-3, the boundary conditions used as described previously, second order descriptions for pressure and second order upwind for momentum, the convergence criterion is set at 10-3 which means the iteration process is said to be convergent if the residual value has reached a value less than 10-3. If convergent results have been achieved, it will proceed to the postprocessing stage, if not, the research will be repeated back to the meshing stage to check whether errors are starting from that stage.

iii. Post-Processing

This stage is the stage where the results and analysis of the results of the iteration process that has been carried out by Ansys are displayed. Qualitative and quantitative results according to Li *et al.,* [16] were obtained, based on the results report that had been determined at the beginning. Quantitative data in the form of pressure distribution coefficient, lift coefficient (Cl), and drag coefficient (Cd), the conditions of velocity distribution streamlines, and pressure distribution contours are shown for qualitative data.

4. Results and Discussion

4.1 Validation

Results from experimental and numeric method (simulation) research were compared and can be seen in Figure 6.

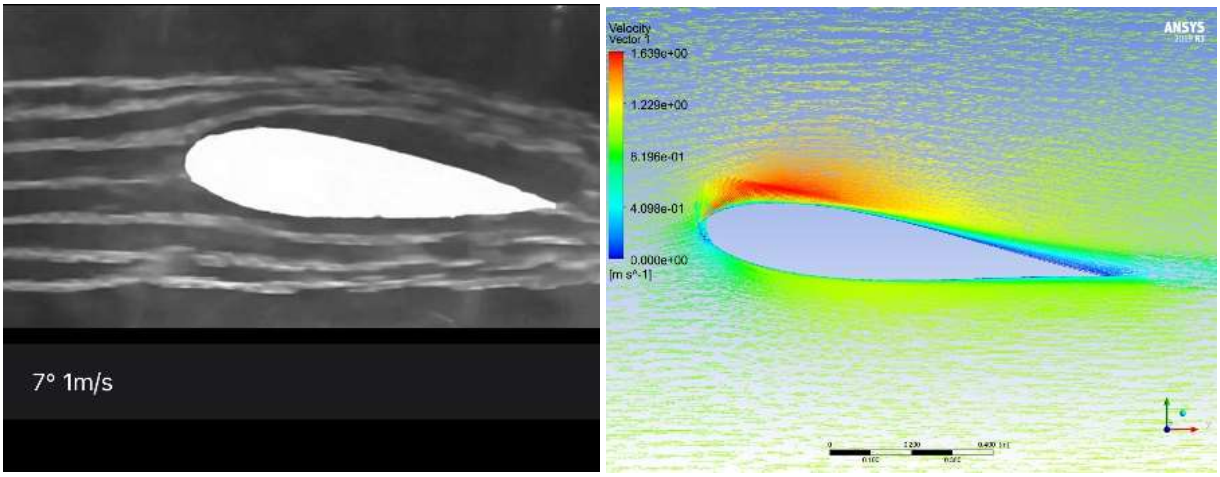

Fig. 6. Comparison between separation flow from experimental research and simulation

In Figure 6, where the flow separation is most clearly seen at an angle of attack of 7° at all velocity values compared to the previous angles of attack, which begins with the presence of a forward saddle point which is the beginning of flow separation in the ground. in front of the leading edge, It can also be seen the color gradation in each image, starting from a speed of 1 m s^{-1} in the red area, where the highest speed occurs at the top of the airfoil with a speed of up to approximately 3 m s^{-1}, in this area the speed reaches the maximum value and the pressure at the minimum value. Then in the middle of the airfoil, there is a gradation of dark blue to light blue where light blue indicates a speed of 0 m s^{-1} (still in the boundary layer area) and light blue shows a speed of approximately 0.7 m s^{-1}.

Following the experimental experiments in a wind tunnel (Figure 7) that have been carried out, with dimensions of Convergence section 80 cm length from 120 cm to 50 cm square, divergence section 180 cm length from 50 cm to 70 cm, and test section 50 cm x 50 cm.

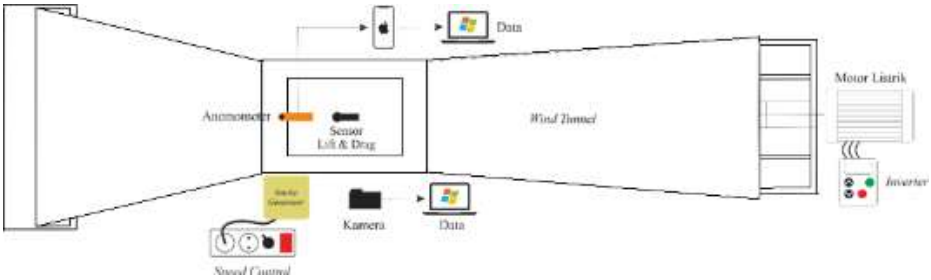

Fig. 7. Wind tunnel with smoke generator

4.2 Coefficient Lift (Cl) and Coefficient Drag (Cd)

One way to understand the characteristics of the airfoil is to know the value of the lift coefficient (Cl) and drag coefficient (Cd). These values can be known through the resultant force acting on the interaction between the fluid and the surface of an object. The lift force is obtained from the resultant force whose direction is perpendicular to the object, while the drag force is obtained from the force parallel to the object. The lift coefficient values obtained in this numerical study (simulation) from the post-processing results on ANSYS can be seen in Figure 8 to Figure 13, which show the value of Cl (lift coefficient) with angles of attack 6°, 7°, and 8° on the airfoil. NACA S1046 with and without a turbulator at speeds of 1 m s^{-1}, to 5 m s^{-1}.

Based on the Figure 8, Figure 9 and Figure 10, it can be seen that the application of a turbulator on the airfoil can increase the lift coefficient value, with the highest lift coefficient value being

relatively different, at an angle of attack of 6° the highest lift coefficient occurs at the turbulator position 50%C with a value of 17.0501, at an angle of attack of 7° the highest lift coefficient occurs at the turbulator position of 50%C with a value of 19.7214, and at an angle of attack of 8° the highest lift coefficient occurs at the turbulator position of 40%C with a value of 22.3432. This can happen because at the placement of a certain turbulator, greater flow momentum is produced to fight against the adverse pressure gradient and shear stress, and at high speeds, the value of the freestream velocity becomes larger. Furthermore, the details of quantitative data on the coefficient of drag.

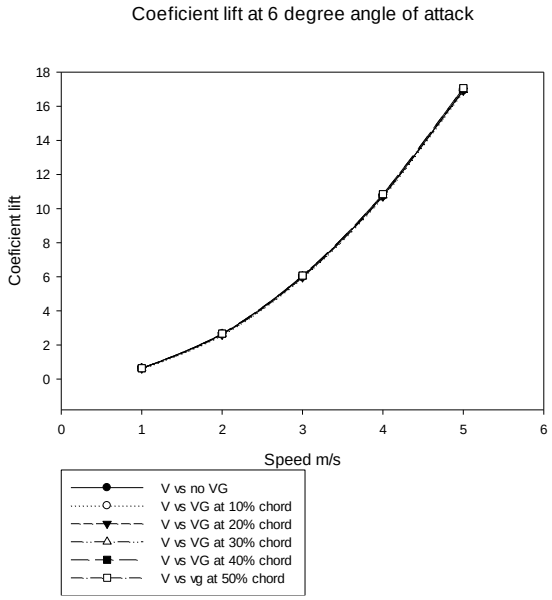

Fig. 8. Graph of comparison of coefficient lift (Cl) values at an AoA 6º

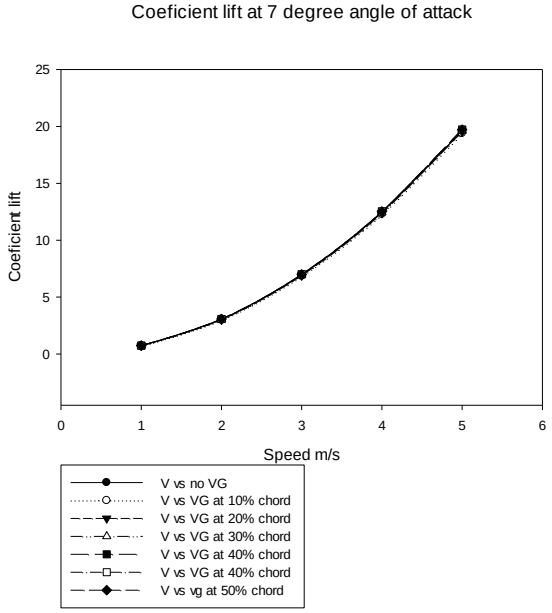

Fig. 9. Graph of comparison of coefficient lift (Cl) values at an AoA 7°

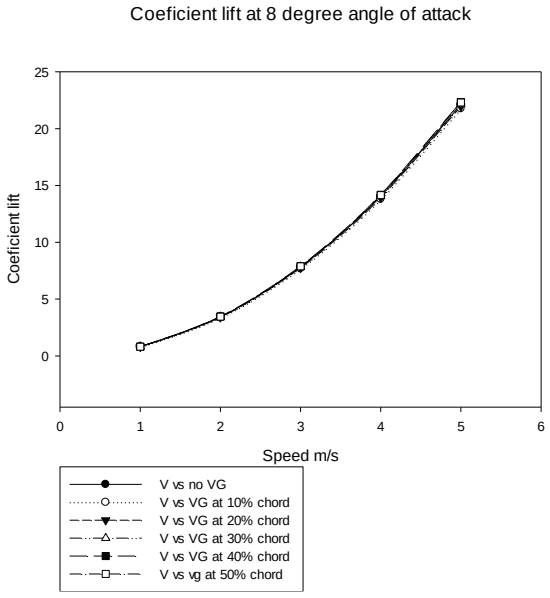

Fig. 10. Graph of comparison of coefficient lift (Cl) values at an AoA 8°

Based on Figure 11, Figure 12 and Figure 13, at each angle of attack and speed, the Cd value in the airfoil with the addition of a turbulator varies, the same as in the lift coefficient. Where the value of the drag coefficient (after the addition of the turbulator) is the smallest at an angle of attack of 6° at positions 50% Chord and 40% Chord, at an angle of attack of 7° at a position of 50% Chord and 40% Chord, and at an angle of attack of 8° the same, namely at the 50% Chord and 40% Chord positions. Despite the increase, the difference between the addition of the most effective turbulator and the no turbulator was not very significant. The value obtained varies due to the placement of a certain turbulator; higher momentum is obtained to fight against the adverse pressure gradient and shear stress. Although both coefficients have increased, there is one more parameter: the ratio of lift and drag coefficients; with this ratio, it can be seen which coefficient has the higher increase.

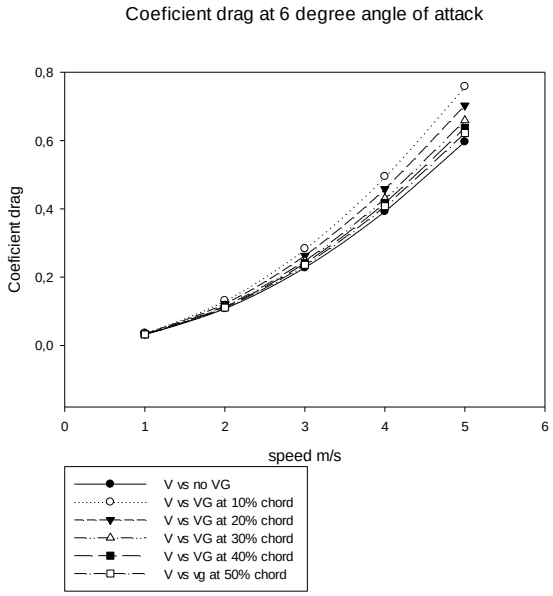

Fig. 11. Graph of comparison of coefficient of drag (Cd) at AoA 6°

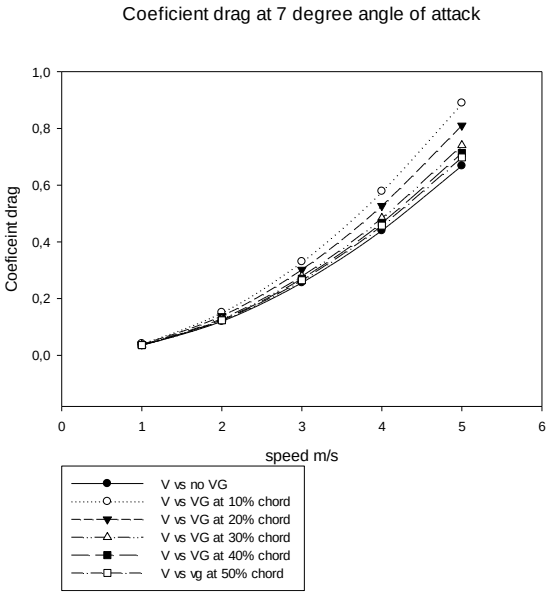

Fig. 12. Graph of comparison of coefficient of drag (Cd) at AoA 7°

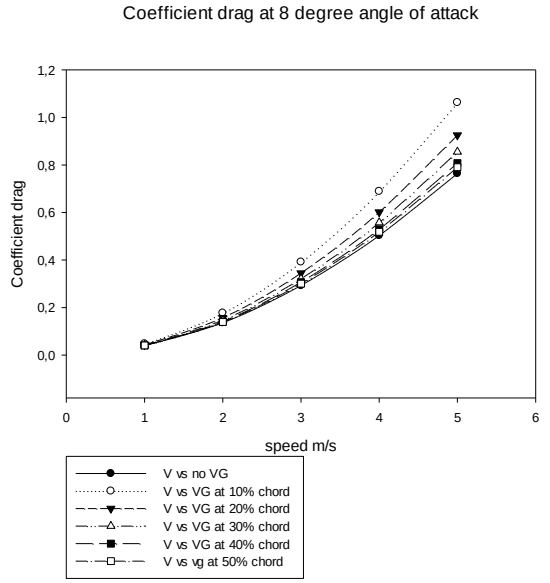

Fig. 13. Graph of comparison of coefficient of drag (Cd) at AoA 8°

4.3 Cl and Cd Ratio (Cl/Cd)

One of the parameters that is also important to evaluate the flow characteristic of the airfoil is the value of (sliding ratio) Cl/Cd [17]. The sliding ratio can be seen in Table 2, Table 3 and Table 4.

Table 2
Sliding Ratio at AoA 6°

V (m/s)	Tanpa VG (6°)	C1/Cd 10% (6°)	C1/Cd 20% (6°)	C1/Cd 30% (6°)	C1/Cd 40% (6°)	C1/Cd 50% (6°)
1	19,9465	16,8898	18,1603	18,1603	19,5306	19,6904
2	24,6356	19,742	21,3631	21,3631	23,5854	24,0803
3	26,463	21,0116	22,6747	22,6747	25,1555	25,734
4	27,4299	21,6241	23,3833	23,3833	25,9569	26,594
5	28,3798	22,2732	24,0685	24,0685	26,7536	27,4363

Table 3
Sliding Ratio at AoA 7°

V (m/s)	Tanpa VG (7°)	C1/Cd 10% (7°)	C1/Cd 20% (7°)	C1/Cd 30% (7°)	C1/Cd 40% (7°)	C1/Cd 50% (7°)
1	20,609	17,114	18,6493	19,8446	20,252	20,2618
2	25,5592	19,7208	21,7559	23,6529	24,5522	24,9666
3	27,2045	20,6833	22,8194	24,9476	25,9251	26,448
4	28,3166	21,2197	23,4695	25,7429	26,821	27,3818
5	29,3387	21,7976	24,1078	26,4846	27,6519	28,2712

Table 4
Sliding Ratio at AoA 8°

V (m/s)	Tanpa VG (7°)	C1/Cd 10% (7°)	C1/Cd 20% (7°)	C1/Cd 30% (7°)	C1/Cd 40% (7°)	C1/Cd 50% (7°)
1	20,2244	16,6323	18,5921	19,6289	20,0491	19,8673
2	25,3019	18,9802	21,6484	23,3682	24,5658	24,8611
3	26,7502	19,5928	22,4895	24,419	25,752	26,2109
4	27,9224	20,0129	23,1378	25,2002	26,7756	27,264
5	28,9602	20,4725	23,727	25,8794	27,6558	28,2055

According to the mentioned data in Table 2 to Table 4, it is evident that the lift and drag coefficient ratio has the smallest ratio value after a turbulator is added at 10% Chord. This is unexpected because the value of the Cl/Cd ratio was much higher before the turbulator was added. This indicates an increase in the drag coefficient value to be greater, even greater the percentage of drag with a turbulator than without a turbulator. In other words, the addition of a turbulator at the 10% Chord position is not effective for the NACA S1046 type airfoil. For the addition of VG/turbulator at 40% Chord and 50% Chord, the value of the Cl/Cd ratio experienced a significant increase at each angle of attack, and this means that the use of a turbulator at 40% Chord and 50% is the most effective placement of the turbulator.

5. Conclusion

Based on the simulation results that have been carried out compared with the experimental results. It can be validated that there is indeed a separation in the airfoil even though the experiment shows that the separation area is larger (at the same speed and angle of attack) compared to the simulation results. Still, the starting point of the separation remains the same, which can occur due to the inadequate quality of the wind tunnel and separation medium. The higher the fluid velocity, the higher the separation area.

To overcome the flow separation phenomenon, a turbulator is designed. The type of turbulator designed is a trapezoidal flat plate counter rotating turbulator with modifications, namely the fillet on the upper right (higher) of 3 mm and the upper left (lower) of 5 mm.

From the simulation result, there is a delay in flow separation with each adjustment of placement, angle, and speed when a qualitative turbulator is added using streamlines and pressure distribution contours visualization. 40% and 50% of the chord is when adding a turbulator has the greatest impact because there is a noticeable rise in Cl. Although there is also an increase in the value of Cd, it is not significant. It can also be seen that the Cl/Cd ratio, where the greater the value of the ratio indicates the greater the value of the lift coefficient than the drag coefficient, and in this study, the largest ratio was found in the placement of the turbulator at 40% of the Cord length and 50% of the Chord length. The turbulator developed in this research will be implemented on the double savonius-darrieus turbine to increasing efficiency.

Acknowledgment
This study received financial support from Universitas Sultan Ageng Tirtayasa's internal research funding for the year 2022. Additionally, we would like to express our gratitude to the Integrated Laboratory of Universitas Sultan Ageng Tirtayasa for providing access to Ansys Fluent Software during the course of this research.

References

[1] Salby, Murry L. "Planetary Waves (Atmospheric Dynamics)." *Encyclopedia of Physical Science and Technology (Third Edition)* (2003): 357-371. https://doi.org/10.1016/B0-12-227410-5/00581-0
[2] Duquesne, Pierre, Joffrey Chanéac, Gabriel Mondin, and Jérôme Dombard. "Topology rule-based methodology for flow separation analysis in turbomachinery." *International Journal of Turbomachinery, Propulsion and Power* 7, no. 3 (2022): 21. https://doi.org/10.3390/ijtpp7030021
[3] Grimshaw, Sam D., James Brind, Graham Pullan, and Ryosuke Seki. "Loss in axial compressor bleed systems." *Journal of Turbomachinery* 142, no. 9 (2020): 091008. https://doi.org/10.1115/1.4047614
[4] Li, Xiao-Bai, Xi-Feng Liang, Zhe Wang, Xiao-Hui Xiong, Guang Chen, Yi-Zheng Yu, and Chun-Mian Chen. "On the correlation between aerodynamic drag and wake flow for a generic high-speed train." *Journal of Wind Engineering and Industrial Aerodynamics* 215 (2021): 104698. https://doi.org/10.1016/j.jweia.2021.104698
[5] Mosbahi, Mabrouk, Mariem Lajnef, Mouna Derbel, Zied Driss, Emanuele Amato, Calogero Picone, Marco Sinagra, and Tullio Tucciarelli. "Effect of the Turbulence Model on the Computational Results of a Lucid Spherical Rotor." *Journal of Advanced Research in Fluid Mechanics and Thermal Sciences* 113, no. 1 (2024): 24-43. https://doi.org/10.37934/arfmts.113.1.2443
[6] Schlichting, Hermann, and Klaus Gersten. "Fundamentals of Boundary-Layer Theory." *Boundary-Layer Theory* (2017): 29-49. https://doi.org/10.1007/978-3-662-52919-5_2
[7] Uppu, Shiva Prasad, and Naren Shankar Radha Krishnan. "Turbulent Airflows over Serrated Wings: A Review on Experimental and Numerical Analysis." *Journal of Advanced Research in Fluid Mechanics and Thermal Sciences* 109, no. 1 (2023): 27-40. https://doi.org/10.37934/arfmts.109.1.2740
[8] Delnero, Juan, Julio Maracyn Di Leo, Mariano Martinez, Federico Bacchi, Jorge Colman Lerner, Ana Scarabino, and Ulfilas Boldes. "Effects of turbulators on airfoil at low Reynolds number in turbulent flow." In *45th AIAA Aerospace Sciences Meeting and Exhibit*, p. 1273. 2007. https://doi.org/10.2514/6.2007-1273
[9] Delnero, Juan Sebastián, Julio Marañon Di Leo, Mauricio Ezequiel Camocardi, Mariano A. Martinez, and Jorge L. Colman Lerner. "Experimental study of vortex generators effects on low Reynolds number airfoils in turbulent flow." *International Journal of Aerodynamics* 2, no. 1 (2012): 50-65. https://doi.org/10.1504/IJAD.2012.046539
[10] Lin, John C. "Review of research on low-profile vortex generators to control boundary-layer separation." *Progress in Aerospace Sciences* 38, no. 4-5 (2002): 389-420. https://doi.org/10.1016/S0376-0421(02)00010-6
[11] Erwin, Erwin, Tresna Priyana Soemardi, Adi Surjosatyo, Sakti Nurfuadi, and Slamet Wiyono. "Performance investigation of dual shaft hybrid vertical turbines using directional fins." *Eastern-European Journal of Enterprise Technologies* 5, no. 8-101 (2019): 53-58. https://doi.org/10.15587/1729-4061.2019.176889
[12] Lusiani, Lusiani, Dhimas Satria, A. B. Rismawan, and Erwin Erwin. "Comparative Study of Damper Effects of Steering Tail Fin Shapes: Part II." In *Conference on Broad Exposure to Science and Technology 2021 (BEST 2021)*, pp. 456-460. Atlantis Press, 2022. https://doi.org/10.2991/aer.k.220131.071
[13] Henrik, Stiesdal, and Vinther Soeren. *The Use of a Turbulator for Damping Stall Vibrations in the Blades of a Wind Turbine*. European Patent Office, EP 0 954 701 B1, 1998.

[14] Muratoğlu, Abdullah, and Muhammed Sungur Demir. "Investigating the Effect of Geometrical and Dynamic Parameters on the Performance of Darrieus Turbines: A Numerical Optimization Approach via QBlade Algorithm." *Bitlis Eren Üniversitesi Fen Bilimleri Dergisi* 9, no. 1 (2020): 413-426. https://doi.org/10.17798/bitlisfen.677137

[15] Rocha, P. A. Costa, H. H. Barbosa Rocha, F. O. Moura Carneiro, M. E. Vieira Da Silva, and A. Valente Bueno. "k-ω SST (shear stress transport) turbulence model calibration: A case study on a small scale horizontal axis wind turbine." *Energy* 65 (2014): 412-418. https://doi.org/10.1016/j.energy.2013.11.050

[16] Li, Xiao-Bai, Xi-Feng Liang, Zhe Wang, Xiao-Hui Xiong, Guang Chen, Yi-Zheng Yu, and Chun-Mian Chen. "On the correlation between aerodynamic drag and wake flow for a generic high-speed train." *Journal of Wind Engineering and Industrial Aerodynamics* 215 (2021): 104698. https://doi.org/10.1016/j.jweia.2021.104698

[17] Nigam, P. K., Nitin Tenguria, and M. K. Pradhan. "Verification of Sliding Ratio (Cl/Cd) of Airfoil through CFD Analysis." *Journal of Scientific Research* 64, no. 1 (2020). https://doi.org/10.37398/JSR.2020.640147